

Spin coherence generation and detection in spherical nanocrystals

M.M. Glazov and D.S. Smirnov

Ioffe Physical-Technical Institute of the RAS, 194021 St-Petersburg, Russia

Theoretical description of electron spin orientation and detection by short optical pulses is proposed for the ensembles of the singly charged semiconductor nanocrystals. The complex structure of the valence band in spherical nanocrystals is taken into account. We demonstrate that the direction of electron spin injected by the pump pulse depends on both the pump pulse helicity and the pump pulse power. It is shown that the train of the optical pulses can lead to the complete orientation of the resident electron spin. The microscopic theory of the spin Faraday, Kerr and ellipticity effects is developed and the spectral sensitivity of these signals is discussed. We show that under periodic pumping the pronounced mode-locking of electron spins takes place and manifests itself as significant spin signals at negative delays between pump and probe pulses.

PACS numbers: 78.67.Hc, 78.47.-p, 71.35.Pq, 75.78.-n, 42.50.Ex

I. INTRODUCTION

One of the most important tasks of semiconductor spintronics, a novel branch of the condensed matter physics aimed at the fundamental and applied research of the charge carriers spin dynamics, is the study of electron and hole spin control by nonmagnetic means [1–4]. In this regard, the manipulation of electron spins by short optical pulses attracts a lot of research attention nowadays [5–8], see Ref. [9] for review.

The spin control is usually realized using the pump-probe technique where a strong circularly polarized pump pulse orients spins of electrons, holes and their complexes and a weak linearly polarized probe pulse monitors their spin polarization via spin (magneto-optical) Faraday, Kerr and ellipticity effects as shown schematically in Fig. 1(a) [10, 11]. Various aspects of the pump-probe technique and features of electron spin dynamics manifested in the pump-probe experiments are reviewed in [1, 2, 12, 13].

Among rich variety of solid-state systems where the pump-probe technique was successfully applied, the structures with singly charged quantum dots are of special importance [1, 13–15]. Ultra-long spin relaxation times in these systems allow one to observe various interesting phenomena including spin precession mode-locking [16] and nuclei-induced spin precession frequency focusing phenomena [17]. Due to these effects about a million of electron spins localized in different dots are coherent and precess synchronously. In most of pump-probe spin dynamics studies the self-assembled quantum dots (quantum disks), where due to the size quantization and strain the ground valence band state is two-fold degenerate and corresponds to the hole spin projections $\pm 3/2$ onto the growth axis, were used. For such structures a microscopic theory of spin Kerr, Faraday and ellipticity effects was developed in Ref. [18]. This theory is in a good agreement with experiments [13, 19].

The aim of the present paper is to address theoretically the processes of the spin coherence generation, control and detection in spherical nanocrystals (NCs) where the

valence band is four-fold degenerate. The specifics of the optical selection rules in this case results in novel qualitative features of spin generation and detection processes absent in the quantum disks. In particular, as shown below, the direction of electron spin initiated by a single pump pulse or by the pump pulse train depends on the pump pulse power: by changing the power of the circularly polarized pump pulse one can generate electron spin oriented either along or in the opposite direction with respect to the light propagation axis. We demonstrate also that the excitation of electron spins by the periodic train of pump pulses can result in the complete orientation of electron spin and in the spin coherence mode-locking if the transverse magnetic field is applied.

The paper is organized as follows. In Sec. II we provide a theoretical description of spin coherence generation in a single nanocrystal under circularly polarized pump pulse. Then in Sec. III we analyze spin dynamics in the external magnetic field and discuss the spin accumulation processes, among them the spin coherence mode-locking. Section IV is divided into two parts, first one is aimed to provide a description of spin Faraday, Kerr and ellipticity signals formation, and the second one presents temporal dependences of spin signals in the nanocrystal arrays. The results are summarized in the Sec. V.

II. SPIN COHERENCE GENERATION

An array of spherical NCs grown of III-V compounds is considered. The NCs are assumed to be singly charged with electrons. The ground state of the dot corresponds to the electron at the lowest single size-quantization level, this state is twofold degenerate with respect to the electron spin projection on a given axis. The excited state we consider is populated as a result of the pump pulse action; it is the singlet trion state, which consists of a pair of electrons with anti-parallel spins and a hole. Hereafter we assume that the optical (carrier) frequencies of the pump, ω_p , and probe, ω_{pr} , pulses are close to the singlet trion resonance frequency, ω_0 , and we neglect therefore all other excited states in the system, e.g. the triplet

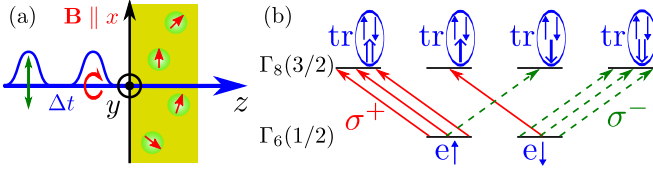


Figure 1. (a) The principal scheme of the pump-probe measurements technique. First (pump) pulse is circularly polarized, and the weak probe pulse is linearly polarized, it arrives at a sample delayed by Δt with respect to the pump pulse. (b) Scheme of optical transitions in the case of degenerate valence band in the charged NC. Transitions under σ^+ (σ^-) polarized pulse are shown by solid (dashed) arrows.

trion.

The singlet trion state degeneracy is determined by the hole spin states. In spherical NCs under study the ground state of the hole transforms according to the Γ_8 representation of T_d point symmetry group. We assume that the radius of the NC R is small enough, $R \ll a_B$, where a_B is exciton Bohr radius, and neglect the Coulomb interaction. Therefore the trion state is fourfold degenerate, and its states can be labelled as $F_z = \pm 3/2, \pm 1/2$. In the spherical (isotropic) approximation F_z is the component of the hole total angular momentum, which includes the orbital momentum of size-quantized state, L , and the angular momentum of Bloch function, J [20–23]. The singlet trion wave function can be written as a product of two-electron function

$$\psi_{ee}(\mathbf{r}_{e1}, \mathbf{r}_{e2}) = f_e(\mathbf{r}_{e1})f_e(\mathbf{r}_{e2}) \frac{|1/2\rangle_1 |-1/2\rangle_2 - |-1/2\rangle_1 |1/2\rangle_2}{\sqrt{2}},$$

where $f_e(\mathbf{r}) = (2\pi r^2 R)^{-1/2} \sin(\pi r/R)$ is the size quantization function of the electron in the limit of infinite barriers, $|s_z\rangle_i$ are the corresponding spinors, and a hole wave function

$$\psi_{h,F_z}(\mathbf{r}_h) = f_0(r_h) |L=0, J=3/2, F=3/2, F_z\rangle + f_2(r_h) |L=2, J=3/2, F=3/2, F_z\rangle,$$

where L is the orbital angular momentum of the hole envelope function, J is the hole spin, and the functions $|L, J, F, F_z\rangle$ are eigenfunctions of the total angular momentum $\mathbf{F} = \mathbf{L} + \mathbf{J}$. Radial functions $f_l(r)$ ($l = 0, 2$) can be expressed in the spherical approximation as [23]

$$f_l(r) = C \left[j_l(\zeta r/R) + (-1)^{l/2} \frac{j_2(\zeta)}{j_2(\sqrt{\beta}\zeta)} j_l(\sqrt{\beta}\zeta r/R) \right],$$

where $j_l(x)$ are the spherical Bessel functions, β is the light to heavy hole mass ratio in the bulk material, ζ is the first root of $j_0(x)j_2(\sqrt{\beta}\zeta) + j_2(x)j_0(\sqrt{\beta}\zeta) = 0$ and C is the normalization constant.

The geometry of the system under study is illustrated in Fig. 1(a). In what follows we choose light propagation axis to be $z \parallel [001]$. The optical selection rules at

the trion resonant excitation are similar to those for the interband absorption in bulk material [24]: under σ^+ polarized pulse action the trions with $F_z = 3/2$ and $1/2$ are formed, while for σ^- pulse the trions with $F_z = -3/2$ and $-1/2$ are formed [25]. Namely, under σ^+ light pulse optical transitions from the electron state with spin projection $S_z = +1/2$ state to the $F_z = +3/2$ trion state and from $S_z = -1/2$ electron state to the $F_z = +1/2$ trion state take place as schematically shown in Fig. 1(b). Similar selection rules with inversion of F_z and S_z signs are relevant for the σ^- pump pulse. Hence, for given pump pulse helicity two optical transitions are involved in contrast with the quantum disk case with simple valence band, considered in [13, 18].

To describe qualitatively the resident electron spin polarization induced by the pump pulse we note that the probabilities to form a trion from $S_z = +1/2$ and $S_z = -1/2$ initial states are different. Indeed, as follows from the symmetry of the system, the ratio of the matrix elements absolute values describing transitions to the states with $|F_z| = 3/2$ and $|F_z| = 1/2$ equals to $\sqrt{3}$ [24]. Therefore, for example, for σ^+ pump the trions are formed more efficiently from $S_z = +1/2$ electrons than from $S_z = -1/2$ ones. Under assumption that hole-in-trion spin relaxation time, τ_s^T , is much smaller than the trion lifetime, τ_{QD} , the electron returning after the trion recombination is unpolarized. As a result the imbalance of $S_z = +1/2$ and $-1/2$ electrons occurs. This model explains the principle of spin orientation of resident electrons in NCs and it is valid only for relatively weak pump pulses. The microscopic theory for arbitrary pump pulse powers is put forward below.

In what follows we assume that the duration of the pump pulse, τ_p , is small enough to neglect the spin precession in an external magnetic field and the recombination and relaxation processes during the pump pulse action: $\tau_p \ll \tau_{QD}, \tau_s^T, T_L, \tau_s$, where τ_s is the electron spin relaxation time in the quantum dot and T_L is the Larmor spin precession period. Hence, it is enough to determine the transformation of electron spin by the pump pulse, and solve afterwards kinetic equations for electron spin dynamics in the interval between the pump pulses [18]. Accordingly, we introduce the six-component wavefunction $\hat{\Psi}$ of the quantum dot:

$$\hat{\Psi} = [\psi_{+1/2}, \psi_{-1/2}, \chi_{+3/2}, \chi_{+1/2}, \chi_{-1/2}, \chi_{-3/2}], \quad (1)$$

where $\psi_{\pm 1/2}$ refer to the resident electron spin states, and four components χ_{F_z} ($F_z = \pm 3/2, \pm 1/2$) refer to the corresponding trion states. It is assumed that the trion states are chosen in the canonical basis for Γ_8 representation of T_d point symmetry group. As described above, the pump pulse with given helicity induces transitions between two electron and two trion states [Fig 1(b)]. Consequently only four components of $\hat{\Psi}$, namely, two electron ones, $\psi_{\pm 1/2}$ and two corresponding trion once will be modified by the pump pulse. The non-stationary Schrödinger equation can be written for the σ^+ polarized

pump pulse as (cf. Refs. [13, 18])

$$i\dot{\chi}_{+3/2} = \omega_0\chi_{+3/2} + \sqrt{3}f(t)e^{-i\omega_p t}\psi_{+1/2}, \quad (2a)$$

$$i\dot{\psi}_{+1/2} = \sqrt{3}f(t)e^{i\omega_p t}\chi_{+3/2}, \quad (2b)$$

$$i\dot{\chi}_{+1/2} = \omega_0\chi_{+1/2} + f(t)e^{-i\omega_p t}\psi_{-1/2}, \quad (2c)$$

$$i\dot{\psi}_{-1/2} = f(t)e^{-i\omega_p t}\chi_{+1/2}. \quad (2d)$$

Here $f(t)$ is a smooth envelope of pump pulse defined as

$$f(t) = -\frac{e^{i\omega_p t}}{\hbar} DE_{\sigma_+}(t), \quad (3)$$

where $E_{\sigma_+}(t) \propto e^{-i\omega_p t}$ is the right circularly polarized component of the electric field of the pump and

$$D = -i\frac{ep_{cv}}{\omega_0 m_0} \frac{1}{\sqrt{4\pi}} \int f_e(r)f_0(r)dr \quad (4)$$

is the dipole matrix element [25] of interband transition between the states $\psi_{-1/2}$ and $\chi_{+1/2}$. In the last expression $e = -|e|$ is the electron charge, m_0 is the free electron mass, and p_{cv} is the interband matrix element of the momentum operator taken between the conduction and valence band Bloch functions at the Γ point of the Brillouin zone. The dependence of electromagnetic field on coordinates is neglected in Eq. (3) since the NC radius is much smaller than the radiation wavelength. Similar to Eqs. 2 set of equations holds for σ^- pump pulse, in which case spins of hole F_z and electron S_z should be inverted.

In pump-probe experiments the generation and detection of electron spin coherence is usually carried out by the train of pump (and probe) pulses following with the repetition period T_R . It exceeds by far the trion lifetime, $T_R \gg \tau_{QD}$. Therefore by the next pump pulse the trion state in the NC is empty, $\chi_{F_z}(t \rightarrow -\infty) \equiv 0$. However, the electron can be, in general, spin polarized. Following Ref. [18] we represent the solution of the system (2) after the pulse is over ($t \gg \tau_p$), as

$$\psi_{+1/2}(t \rightarrow +\infty) = Q_+ e^{i\Phi_+} \psi_{+1/2}(t \rightarrow -\infty), \quad (5a)$$

$$\psi_{-1/2}(t \rightarrow +\infty) = Q_- e^{i\Phi_-} \psi_{-1/2}(t \rightarrow -\infty). \quad (5b)$$

Here $Q_{\pm} \in [0; 1]$ and $\Phi_{\pm} \in (-\pi; \pi]$ are the parameters, which depend on the shape, power and carrier frequency of the pump pulse. The key difference of the present result, Eqs. (5), from the case of simple valence band, considered in Ref. [13, 18] is the fact that the both electron spin components are transformed under the pump pulse action. Equations (5) allow one to relate the electron spin components before the pulse, $\mathbf{S}^- = (S_x^-, S_y^-, S_z^-)$, and after the pulse, $\mathbf{S}^+ = (S_x^+, S_y^+, S_z^+)$, as follows:

$$S_z^+ = \frac{Q_+^2 - Q_-^2}{4} + \frac{Q_+^2 + Q_-^2}{2} S_z^-, \quad (6a)$$

$$S_x^+ = Q \cos \Phi S_x^- + Q \sin \Phi S_y^-, \quad (6b)$$

$$S_y^+ = Q \cos \Phi S_y^- - Q \sin \Phi S_x^-, \quad (6c)$$

where $Q = Q_+ Q_-$ and $\Phi = \Phi_+ - \Phi_-$. It follows from Eqs. (6), that the electron spin pseudovectors before the pump pulse and after it are connected linearly. In accordance with Eq. (6a) the pump pulse generates z -spin component (first term) and transforms the already present one (second term). The spin components in the plane perpendicular to the light propagation axis are reduced due to the factor Q in Eqs. (6b) and (6c) and are rotated around z -axis by the angle Φ . Similar to Eq. (6) relations hold also for σ^- pump pulse, in which case $Q_+(\Phi_+)$ and $Q_-(\Phi_-)$ should be swapped.

To simplify the following discussion, we assume that the hole-in-trion spin relaxation is fast as compared with the radiative lifetime of the trion. In this case, the carrier returning after the trion recombination is completely depolarized and the long-living spin coherence generation is governed by Eqs. (6). Otherwise, to determine the resident electron spin induced by the pump pulse one has to solve the full system of spin dynamics equations taking into account both electron and trion spins, cf. Refs. [26–28].

Let us consider an important limiting case of resonant pump pulse, where $\omega_p = \omega_0$. It can be shown, that $\Phi_{\pm} = 0$ and Q_{\pm} are expressed via the effective pump area $\Theta = 2 \int_{-\infty}^{\infty} f(t)dt$ [13] as

$$Q_+ = \cos\left(\frac{\sqrt{3}\Theta}{2}\right), \quad Q_- = \cos\left(\frac{\Theta}{2}\right), \quad (7)$$

The periodic dependence of Q_+ and Q_- on Θ is related to the Rabi oscillations taking place in two-level systems corresponding to optical transitions between electron state with $S_z = +1/2$ and the trion state with $F_z = +3/2$, and between the electron state $S_z = -1/2$ and $F_z = +1/2$ trion. The periods of these oscillations are incommensurable due to the irrational ratio of the corresponding matrix elements ($\sqrt{3}$). It results in the non-periodic dependence of the electron spin z component generated by the single pump pulse $S_z^{(1)} = [\sin^2(\Theta/2) - \sin^2(\sqrt{3}\Theta/2)]/4$ on pulse area (cf. Ref. [29]). This dependence is shown by the solid line in Fig. 2(a). For comparison, the dashed line in Fig. 2(a) shows the electron spin z component in the model of simple valence band structure, $-\sin^2(\sqrt{3}\Theta/2)/4$ [18]. In both cases $|S_z| \leq 1/4$, because in the “best” case, one of two-level systems gets into the excited state, while the other one remains in the ground state [18]. Interestingly, that for the spherical NC considered here, depending on the pump pulse area Θ either the transition related with electron with $S_z = +1/2$ or the one with $S_z = -1/2$ can dominate. Hence, the electron spin after the pump pulse with given helicity can be directed parallel or antiparallel to z axis depending on Θ by contrast to the self-organized quantum dots with the simple valence band.

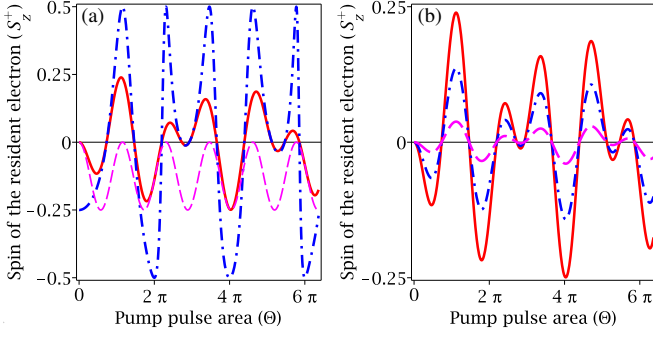


Figure 2. (a) The spin of the resident electron in the NC generated after a single σ^+ pump pulse (red/solid line) and after the train of such pulses (blue/dot-dashed line) as functions of the pump pulse area Θ at zero magnetic field. Resident electron spin in the quantum disk after a single pulse $S_z = -\sin^2(\sqrt{3}\Theta/2)/4$ is presented by thin magenta/dashed line. (b) Resident electron spin after a single Rosen and Zener pump pulse for different detunings between the pump optical frequency and NC transition frequency $[(\omega_0 - \omega_p)\tau_p/(2\pi) = 0, 0.25, 0.5$ for red/solid, blue/dash-dotted and magenta/dashed curves, respectively].

Now let us briefly consider the case of non-resonant pumping. In order to obtain an analytic solution we consider the Rosen and Zener shape of the pump pulse:

$$f(t) = \frac{\mu}{\text{ch}(\pi t/\tau_p)},$$

where the parameter μ determines the pulse area $\Theta = 2\mu\tau_p$. Following Ref. [18] we obtain for Q_{\pm} and Φ_{\pm} :

$$Q_{\pm} = \sqrt{1 - \frac{\sin^2(\Theta_{\pm}/2)}{\text{ch}^2(\pi y)}}, \quad (8)$$

$$\Phi_{\pm} = \arg \left\{ \frac{\Gamma^2(\frac{1}{2} - iy)}{\Gamma(\frac{1}{2} - \frac{\Theta_{\pm}}{2\pi} - iy) \Gamma(\frac{1}{2} + \frac{\Theta_{\pm}}{2\pi} - iy)} \right\}, \quad (9)$$

where $\Theta_+ = \sqrt{3}\Theta_- \equiv \sqrt{3}\Theta$, and $y = (\omega_p - \omega_0)\tau_p/(2\pi)$ is the dimensionless detuning. It follows from Eqs. (6a) and (8) that the electron spin z component induced by a single detuned pump pulse has the form

$$S_z^{(1)}(\Theta, y) = \frac{S_z^{(1)}(\Theta, 0)}{\text{ch}^2(\pi y)} = \frac{\sin^2(\Theta/2) - \sin^2(\sqrt{3}\Theta/2)}{4 \text{ch}^2(\pi y)}, \quad (10)$$

and decreases monotonously with an increase of the detuning, $|y|$. This dependence is illustrated in Fig 2(b), where different curves correspond to different values of $y = 0, 0.25, 0.5$. Overall dependence of $S_z^{(1)}(\Theta, y)$ is the same for all detunings in the case of Rosen and Zener pump pulse.

It is worth noting that for the deformed NC of elliptic shape or in NC made of the wurzite semiconductor,

the transitions involving $S_z = +1/2$ and $S_z = -1/2$ electrons are characterized by different detunings, in general. It results in even more complex dependence of $S_z^{(1)}$ on the pump pulse area. In the particular case, where the splitting between $|F_z| = 3/2$ and $|F_z| = 1/2$ trion states exceeds by far the spectral width of pump pulse \hbar/τ_p only one optical transition can be excited and spin orientation is described by the model of [18]. In the opposite case the model presented here is valid. Hence, by choosing appropriate pulse spectral width and strength one can orient spin in arbitrary direction for nanocrystal systems like studied in Refs. [30, 31].

III. SPIN ACCUMULATION CAUSED BY THE TRAIN OF PUMP PULSES

In the pump-probe Faraday and Kerr rotation experiments the sample is usually subjected to a train of pump pulses that follow with a certain repetition period T_R . We assume that T_R exceeds by far the radiative lifetime of a trion in a quantum dot, τ_{QD} , but it may be comparable or smaller than the single electron spin relaxation time in a QD, $T_R \leq \tau_{s,e}$. In this case, the electron spin retains the memory of being exposed to the previous pulses, resulting in the resonant spin amplification and spin mode-locking effects [16, 32].

Let us consider firstly the simple case, where the external magnetic field is absent, $\mathbf{B} = 0$. For simplicity we assume also that the electron spin relaxation time exceeds by far the pump pulse repetition period. Hence, electron spin is conserved between the pump pulses and $\mathbf{S}^+ = \mathbf{S}^-$ in the steady state. As a result for the electron spin components after the sufficiently long train of the pump pulses we obtain

$$S_x^+ = S_x^- = S_y^+ = S_y^- = 0, \quad (11a)$$

$$S_z^+ = S_z^- = \frac{Q_+^2 - Q_-^2}{4 - 2(Q_+^2 + Q_-^2)}. \quad (11b)$$

The dependence of electron spin S_z component accumulated by the train of the pump pulses and calculated after Eqs. (11) is shown in Fig. 2(a) by the dash-dotted line. Interestingly, that for the Rosen and Zener pump pulse shape, the dependence of S_z on the pump pulse area is independent of the detuning between the pump pulse frequency and the quantum dot transition frequency, as follows from Eqs. (8) and (11). We have checked that this dependence is weak for rectangular-shaped pulse.

It is noteworthy that the electron spin polarization may reach 100% for spherical NC. This is in contrast to the classical optical orientation regime in the systems with Γ_8 symmetry of the valence band, where up to 50% spin polarization can be realized. Such an enhancement of spin polarization and the dependence of the electron spin direction on the pump pulse area is related with the two-level nature of the optical transitions in NCs. For

example, if one of the two-level systems (associated with the $F_z = +3/2$ or $F_z = +1/2$) trion is inactive, which happens if $Q_+ = 1$ or $Q_- = 1$, only electrons with the fixed spin component are depolarized ($S_z = 1/2$ or $-1/2$, respectively). Such a situation is similar to the one considered in Refs. [18, 33]. As a result, the sufficiently long train of pump pulse brings completely erases one electron spin component, hence, resident carriers become fully polarized.

In the general case, where the magnetic field is applied to the NC, the resident electron spin dynamics is governed by the following equation:

$$\frac{d\mathbf{S}}{dt} + \mathbf{S} \times \boldsymbol{\Omega}_L + \frac{\mathbf{S}}{\tau_{s,e}} = 0. \quad (12)$$

The equation takes into account the electron spin relaxation processes and the precession of electron spins in the magnetic field \mathbf{B} with the frequency $\boldsymbol{\Omega}_L = g_e \mu_B \mathbf{B}$, where

g_e is the electron Landé factor and μ_B is the Bohr magneton. Following Refs. [18, 28] we obtain the following steady-state expressions for the electron spin components \mathbf{S}^- right before the pump pulse arrival

$$S_x^- = K S_y^-, \quad (13a)$$

$$S_y^- = \frac{Q_-^2 - Q_+^2}{4\Delta} e^{-T_R/\tau_{s,e}} \sin(\Omega_L T_R), \quad (13b)$$

$$S_z^- = \frac{Q_-^2 - Q_+^2}{4\Delta} e^{-T_R/\tau_{s,e}} \times \left[Q(\cos \Phi - K \sin \Phi) e^{-T_R/\tau_{s,e}} - \cos(\Omega_L T_R) \right], \quad (13c)$$

where

$$\Delta = 1 - e^{-T_R/\tau_{s,e}} \left[\frac{Q_+^2 + Q_-^2}{2} + Q(\cos \Phi - K \sin \Phi) \right] \cos(\Omega_L T_R) + \frac{Q(Q_+^2 + Q_-^2)}{2} e^{-2T_R/\tau_{s,e}} (\cos \Phi - K \sin \Phi), \quad (14a)$$

$$K = \frac{Q e^{-T_R/\tau_{s,e}} \sin \Phi}{1 - Q e^{-T_R/\tau_{s,e}} \cos \Phi}. \quad (14b)$$

We remind that $Q = Q_+ Q_-$. In the limit of $Q_- = 1$, i.e. where one of the two level systems is inactive Eqs. (13) pass to those obtained in Ref. [18] for the simple valence band system.

In order to analyze Eqs. (13) we consider an important limiting case of resonant pumping, where $\Phi = 0$, and neglect completely the resident electron spin relaxation ($\tau_{s,e} \rightarrow \infty$). This results in $K = 0$,

$$\Delta = 1 - \left[\frac{Q_+^2 + Q_-^2}{2} + Q \right] \cos \Omega_L T_R + \frac{Q(Q_+^2 + Q_-^2)}{2}, \quad (15)$$

see Eqs. (14a), (14b), and leads to the following simplified expressions for the electron spin components accumulated by the train of the pump pulses:

$$S_x^- = 0, \quad (16a)$$

$$S_y^- = \frac{Q_-^2 - Q_+^2}{4\Delta} \sin \Omega_L T_R, \quad (16b)$$

$$S_z^- = \frac{Q_-^2 - Q_+^2}{4\Delta} [Q - \cos \Omega_L T_R]. \quad (16c)$$

Clearly, $S_x \equiv 0$ for the considered geometry, since the magnetic field is parallel to x axis and optical pulses do not lead to the spin rotation in (xy) plane in the resonant case.

Under the phase synchronization condition [16, 17, 28, 32, 34–36],

$$\Omega_L T_R = 2\pi N, \quad N = 0, 1, 2, \dots, \quad (17)$$

the spin of electron makes an integer number of turns between the subsequent pump pulses and the electron spin is given by the same expressions as in the absence of the magnetic field, see Eqs. (11) and may reach $\pm 1/2$ depending on pump pulse area.

For weak pump pulses, where the pulse area $\Theta \ll 1$ one obtains

$$S_z^- \approx \frac{\Theta^2}{16} \times \left(1 - \frac{(2 + \cos \Omega_L T_R) \Theta^2}{3[(1 - \cos \Omega_L T_R)(2 - \Theta^2) + (41 - 17 \cos \Omega_L T_R) \frac{\Theta^4}{96}]} \right), \quad (18)$$

$$S_y^- \approx \frac{\Theta^2}{8} \frac{\sin \Omega_L T_R}{(1 - \cos \Omega_L T_R)(2 - \Theta^2) + (41 - 17 \cos \Omega_L T_R) \frac{\Theta^4}{96}}.$$

Note, that the peaks of the dependence of S_z on magnetic field corresponding to the phase synchronization condition (17) are very sharp. If the spin relaxation and the detuning are completely neglected, their width is determined by the pump pulse area ($\sim \Theta^2$), otherwise it is

determined by ratio $T_R/\tau_{s,e} \ll 1$ or $|\Phi|$, whichever is larger, see Ref. [18] for details. In the resonant case the electron spin z -component equals to $-1/4$ like in the bulk system with Γ_8 symmetry since a train of weak pulses is similar to the *cw* pumping of the bulk material.

In the other important case, where Q_+ or $Q_- = 0$ the corresponding two-level system is excited to the trion state with a unit probability. In this limit $Q = 0$, and the electron spin components take very simple form:

$$S_x^- = 0, \quad S_y^- = -\frac{Q_+^2}{4\Delta} \sin \Omega_L T_R, \quad (19a)$$

$$S_z^- = \frac{Q_+^2}{4\Delta} \cos \Omega_L T_R, \quad (19b)$$

where $\Delta = 1 - \cos(\Omega_L T_R)Q_+^2/2$ and we assumed that $Q_- = 0$ for the sake of definiteness. In this situation under the synchronization condition (17) the electron spin becomes fully polarized.

IV. PROBING THE ELECTRON SPIN IN QUANTUM DOTS

A. Formation of spin Faraday and ellipticity signals in NC

The detection of the QD spin polarization in pump-probe Faraday and Kerr rotation experiments is carried out by a weak linearly polarized probe pulse. The electric field of the probe pulse oscillates along the x axis and can be written as

$$\mathbf{E}^{pr}(\mathbf{r}, t) = E_x^{pr}(\mathbf{r}, t)\mathbf{o}_x + c.c.$$

Here we assume that $E_x^{pr}(\mathbf{r}, t) = E_0 s(t)e^{-i\omega_{pr}t}$, where ω_{pr} is the carrier frequency of the probe beam, E_0 is the probe pulse amplitude, $s(t)$ is its smooth envelope, and \mathbf{o}_i ($i = x, y, z$) is the unit vector along i th axis. The Faraday signal \mathcal{F} detected in the transmission geometry can be written as [13, 18]

$$\mathcal{F} = \lim_{z \rightarrow +\infty} \int \left[\left| E_{x'}^{(t)}(z, t) \right|^2 - \left| E_{y'}^{(t)}(z, t) \right|^2 \right] dt, \quad (20)$$

where x', y' axes are oriented at 45° with respect to the initial reference frame x, y ; $E_{x'}^{(t)}(z, t)$ and $E_{y'}^{(t)}(z, t)$ are the components of the transmitted field. Kerr rotation signal can be presented similarly to Eq. (20) with the replacement of the transmitted fields by the reflected ones. Similarly, the ellipticity of the transmitted beam reads

$$\mathcal{E} = \lim_{z \rightarrow +\infty} \int \left[\left| E_{\sigma^+}^{(t)}(z, t) \right|^2 - \left| E_{\sigma^-}^{(t)}(z, t) \right|^2 \right] dt. \quad (21)$$

Here the subscripts σ^+ and σ^- correspond to the circular components of the transmitted light.

In order to find the transmitted and reflected electromagnetic field we follow the procedure developed in Refs. [13, 18] and calculate response of the NC to the linearly polarized probe field. To that end, the electric field of the probe pulse is decomposed in a superposition of circularly polarized waves and system (2) and its counterpart for other circular polarization are used to determine the change of the quantum dot wavefunction. Corresponding equations are solved in the first order in electric field \mathbf{E}^{pr} [37]. Afterwards the dielectric polarization of the NC is calculated and the re-emitted field is determined from the Maxwell equations. The resulting expressions for spin Faraday and ellipticity signals for the three-dimensional (bulk) array of NCs read:

$$\mathcal{E} + i\mathcal{F} = \quad (22)$$

$$\frac{\pi N_{NC} L}{q^2 \tau_{NC}} |E_0|^2 \left[J_z + i \langle \{J_x, J_y\}_s \rangle - 2S_z \right] G(\omega_{pr} - \omega_0).$$

Here $q = \omega_{pr} \sqrt{\varepsilon_b}/c$ is the radiation wavevector in the medium, ε_b is the dielectric constant of the matrix, which is assumed to coincide with the background dielectric constant of the NCs,

$$\tau_{NC} = \frac{3\hbar c^3}{4|D|^2 \omega_0^3 \varepsilon_b}$$

is the radiative lifetime of an electron-hole pair confined in the NC [25], N_{NC} is the (volume) density of the NC, L is the thickness of the array. Complex-valued function $G(\omega_{pr} - \omega_0)$ in Eq. (22) determines the spectral sensitivity of the spin Faraday and ellipticity signals [13, 18]

$$G(\Lambda) = \int_0^\infty dt e^{i\Lambda t} \int_{-\infty}^\infty dt' s(t') s(t + t').$$

The explicit expressions for $G(\Lambda)$ are given by Eq. (61) of Ref. [18] for different probe pulse shapes. Its real and imaginary parts for the case of Rozen & Zener pulse are shown by red dashed and blue dotted lines in Fig. 3(a), respectively. It is noteworthy, that the spin Kerr signal is a superposition of spin Faraday and ellipticity signals with the coefficients determined by phase acquired by the probe pulse in the cap layer [13, 18].

Quantities S_z and J_z in Eq. (22) are the electron and the hole-in-trion z -spin components at the moment of the probe pulse arrival. The probe pulse duration is assumed to be short as compared with all other time scales in the system, and therefore, the electron spin can be considered as frozen during the probe pulse action. Interestingly, the Faraday rotation and ellipticity signals contain contribution from the quantity $\langle \{J_x, J_y\}_s \rangle$, which is the quantum mechanical average of the symmetrized product of J_x, J_y hole spin operators, $\{J_x, J_y\}_s = (J_x J_y + J_y J_x)/2$. Note, that the similar combination of electron spin operators (although being symmetry allowed) does not contribute to the spin Faraday and ellipticity effects since second powers of electron spin operators reduce to the first powers [38]. The contributions due to the trion spin polarization vanish if the pump-probe delay exceeds τ_{NC} , the

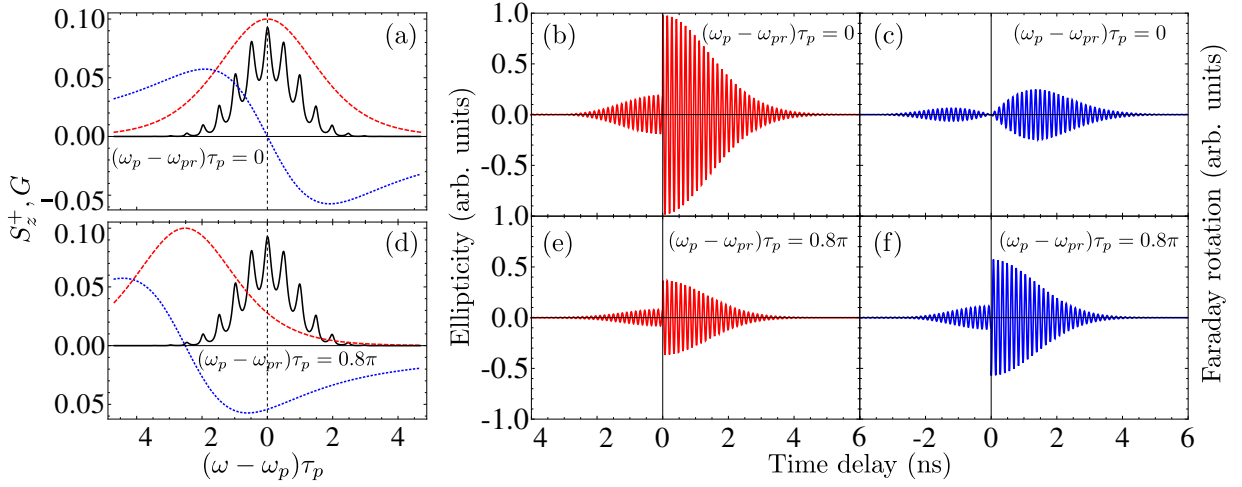


Figure 3. (a) Electron spin polarization, S_z^+ , created by a train of Rozen & Zener σ^+ polarized pump pulses with the repetition period $T_R = 13.2$ ns, as a function of NC optical transition frequency ω_0 (black/solid line). The real (red/dashed) and imaginary (blue/dotted) parts of function $G(\omega - \omega_p)$ are shown in panels (a) and (d). Panels (b,c) represent the time resolved dependence of the spin ellipticity and Faraday rotation signals in the QD ensemble for the degenerate pump-probe regime ($\omega_p = \omega_{pr}$). Panels (d) – (f): same as in (a) – (c), but for the nondegenerate regime ($\omega_p - \omega_{pr})\tau_p = 0.8\pi$. Calculations are carried out for the pump pulses of the area $\Theta = \pi$, the in-plane magnetic field $B = 1$ T, $\tau_p = 100$ fs, $\tau_{s,e} = 1$ μ s, $\hbar\bar{\omega}_0 = 1.4$ eV, $\hbar\Delta\omega_0 = 6.15$ meV [16]. Parameters A and C in Eq. (24) are: $A = -1.75$ eV $^{-1}$, $C = 2.99$ [16].

radiative lifetime of an electron-hole pair is the nanocrystal, therefore pump-probe signals at long enough delays are determined by the electron spin z component only. It is assumed below that the pump-probe delay exceeds the trion lifetime in the NC and we focus solely on the electron spin contribution to the Faraday and ellipticity signals.

We note, that due to the degeneracy of the heavy- and light-hole states the spin Faraday, Kerr and ellipticity signals are proportional to the electron spin projection onto the light propagation axis. Hence, by changing the direction of light propagation one can study the dynamics of all spin pseudovector components, making spherical nanocrystals most suitable for the spin state tomography measurements [39].

Before we proceed with the discussion of spin Faraday and ellipticity signals temporal behavior, let us estimate the typical spin signal strengths. For the NC array with a concentration $N_{NC} = 10^{15}$ cm $^{-3}$, thickness $L = 10^{-4}$ cm the Faraday rotation angle can be estimated according to Eq. (20) as ~ 10 mrad for $\tau_{NC} = 400$ ps, $\hbar\bar{\omega}_0 = 1.4$ eV, $\varepsilon_b = 11$.

B. Temporal dependence of spin Faraday and ellipticity signals

In real NC ensembles the optical transition energies and electron Larmor precession frequencies vary. To simulate the spin signals of such inhomogeneous array of NCs we consider a normal distribution of resonant transition frequencies in NCs, ω_0 , around a certain mean value $\bar{\omega}_0$

with a dispersion $\Delta\omega_0$ [18]

$$\rho(\omega_0) = \frac{1}{\sqrt{2\pi}(\Delta\omega_0)^2} \exp\left[-\frac{(\omega_0 - \bar{\omega}_0)^2}{2(\Delta\omega_0)^2}\right]. \quad (23)$$

The electron spin precession frequency is determined both by the electron g -factor and by the fluctuations of nuclei spins, the latter are neglected hereinafter for simplicity. The main contribution to the g -factor spread is related with its variation with the band gap, see Refs. [19, 40, 41] for details. Under the conditions that $\Delta\omega_0 \ll \bar{\omega}_0$ the dependence of the g -factor on the resonance frequency can be taken in the linear form,

$$g_e(\omega_0) = A\hbar\omega_0 + C, \quad (24)$$

where A and C are some coefficients. In accordance with Eq. (22) the electron spin Faraday and ellipticity signals as functions of the time-delay between the probe and the pump pulses t in the quantum dot ensemble are given by (cf. Refs. [13, 19])

$$\mathcal{E} + i\mathcal{F} = -2\frac{\pi N_{NC}L}{q^2\tau_{NC}}|E_0|^2 \int S_z(\omega_0, \omega_p; t)G(\omega_{pr} - \omega_0)\rho(\omega_0)d\omega_0. \quad (25)$$

where $S_z(\omega_0, \omega_p; t)$ is the temporal dependence of the electron spin in the quantum dot with the resonance frequency ω_0 induced by the pump with the carrier frequency ω_p , which can be found from Eqs. (12) and (13). The variation of the τ_{NC} with the variation of resonance frequency is neglected in Eq. (25) since this dependence is very smooth on the scale of the inverse pulse duration.

The spread of spin precession frequencies caused by the g -factor spread gives rise to important consequences.

First, for some quantum dots in the ensemble the spin precession frequency and the pump pulse repetition frequency are commensurable, see Eq. (17), resulting in the strong enhancement of the S_z in these dots. The distribution of the electron spin z -component right after the pump pulse arrival as a function of the quantum dot optical transition frequency is shown by the solid curve in Fig. 3(a),(d). The peaks on these curve correspond to the dots which satisfy the phase synchronization condition (17). This yields the mode-locking of electron spin precession [16]: the total spin of the ensemble induced by the pump pulse gets dephased due to the spread of the spin precession frequencies on the nanosecond time scale, and before the next pulse arrival the spin polarization of ensemble emerges due to the contribution of the nanocrystals where the spin precession is synchronized. This is clearly seen in Figs. 3(b),(c),(e) and (f), where the temporal dependence of the spin ellipticity [(b), (e)] and Faraday rotation [(c), (f)] are presented for different detunings between the pump and probe pulses. It is worth to stress, that the allowance for the nuclei-induced electron frequency effect can result in even higher amplitudes of the signals at negative delays [17, 34, 35].

Second consequence of the g -factor spread is clearly manifested in Fig. 3(c) where the Faraday rotation signal for degenerate pump and probe pulses is demonstrated. Notably, the Faraday rotation is absent at $t = 0$, and the signal amplitude is a non-monotonous function of the time delay: firstly it grows with time and afterwards it decays. This is a feature of the spectral sensitivity of the Faraday effect which is described by the odd function of the detuning, see blue dotted curve in Fig. 3(a). The dependence of electron spin z -component on the detuning, $\omega - \omega_p$, is symmetric right after the pump pulse arrival ($t = 0$) but becomes asymmetric as time goes by due to the correlation of electron g -factor and the resonance frequency of the NC. It results in the growth of the Faraday rotation signal with time. For even higher time delays the Faraday rotation amplitude decays due to the spin dephasing [19]. The pump-probe detuning itself introduces the asymmetry of the spin distribution with respect to the probe frequency, see Fig. 3(d) and the

Faraday rotation signal shows the behaviour similar to that of the ellipticity, namely, damped oscillations. The interaction of electron spins with nuclei may result in the breaking of the direct link of the electron spin precession frequency and optical transition frequency making the growth of spin Faraday signal less pronounced.

V. CONCLUSIONS

In the present work the microscopic description of the resident electron spin dynamics under the pump-probe conditions in spherical nanocrystals is developed. It is shown, that the complex structure of the valence band allows one to control the magnitude and direction of the resident electron spin in the nanocrystal by means of the pump power variation. It results from the possibility to activate or suppress two possible optical transition paths, involving heavy and light holes. We have demonstrated that the periodic pumping can result in the pronounced spin coherence mode-locking and lead to the complete polarization of electron spins by sufficiently long trains of the pump pulses.

Spin Faraday and ellipticity signals were calculated for the three-dimensional inhomogeneous arrays of nanocrystals. It was shown that the signals possess information on electron and hole spin dynamics, moreover, due to the ensemble inhomogeneity the temporal behavior of the Faraday and ellipticity effects can be different.

The results of this work can be also applied to the description of spin coherence generation and detection for electrons in colloidal nanocrystals or for electrons localized on donors in the bulk GaAs-type semiconductors where the donor-bound exciton can be optically excited.

ACKNOWLEDGMENTS

We thank A. Grelich, E.L. Ivchenko, D.R. Yakovlev and I.A. Yugova for valuable discussions. Financial support of RFBR, RF President Grant NSh-5442.2012.2, and EU projects Spinoptronics and POLAPHEN is gratefully acknowledged.

-
- [1] *Spin Physics in Semiconductors*, edited by M. I. Dyakonov (Springer-Verlag: Berlin, Heidelberg, 2008)
 - [2] *Semiconductor Science and Technology, Special Issue: Optical Orientation*, edited by Y. Kusraev and G. Landwehr, Vol. 23 (IOP Publishing, 2008)
 - [3] D. D. Awschalom and M. E. Flatté, *Nat. Phys.* **3**, 153 (2007)
 - [4] M. Wu, J. Jiang, and M. Weng, *Physics Reports* **493**, 61 (2010)
 - [5] A. J. Ramsay, S. J. Boyle, R. S. Kolodka, J. B. B. Oliveira, J. Skiba-Szymanska, H. Y. Liu, M. Hopkinson, A. M. Fox, and M. S. Skolnick, *Phys. Rev. Lett.* **100**,

- 197401 (2008)
- [6] C. Phelps, T. Sweeney, R. T. Cox, and H. Wang, *Phys. Rev. Lett.* **102**, 237402 (2009)
- [7] A. Grelich, S. E. Economou, S. Spatzek, D. R. Yakovlev, D. Reuter, A. D. Wieck, T. L. Reinecke, and M. Bayer, *Nature Physics* **5**, 262 (2009)
- [8] E. A. Zhukov, D. R. Yakovlev, M. M. Glazov, L. Fokina, G. Karczewski, T. Wojtowicz, J. Kossut, and M. Bayer, *Phys. Rev. B* **81**, 235320 (2010)
- [9] A. J. Ramsay, *Semiconductor Science and Technology* **25**, 103001 (2010)

- [10] D. D. Awschalom, J. M. Halbout, S. von Molnar, T. Siegrist, and F. Holtzberg, *Phys. Rev. Lett.* **55**, 1128 (1985)
- [11] N. I. Zheludev, M. A. Brummell, R. T. Harley, A. Malinowski, S. V. Popov, D. E. Ashenford, and B. Lunn, *Solid State Commun.* **89**, 823 (1994)
- [12] T. Korn, *Physics Reports* **494**, 415 (2010)
- [13] M. M. Glazov, *Fiz. Tverd. Tela* **54**, 3-27 (2012) [Engl. transl.: *Phys. of the Solid State* **54**, 1 (2012)]
- [14] M. H. Mikkelsen, J. Berezovsky, N. G. Stoltz, L. A. Coldren, and D. D. Awschalom, *Nat. Physics* **3**, 770 (2007)
- [15] M. Atature, J. Dreiser, A. Badolato, and A. Imamoglu, *Nature Physics* **3**, 101 (2007)
- [16] A. Greilich, D. R. Yakovlev, A. Shabaev, A. L. Efros, I. A. Yugova, R. Oulton, V. Stavarache, D. Reuter, A. Wieck, and M. Bayer, *Science* **313**, 341 (2006)
- [17] A. Greilich, A. Shabaev, D. R. Yakovlev, A. L. Efros, I. A. Yugova, D. Reuter, A. D. Wieck, and M. Bayer, *Science* **317**, 1896 (2007)
- [18] I. A. Yugova, M. M. Glazov, E. L. Ivchenko, and A. L. Efros, *Phys. Rev. B* **80**, 104436 (2009)
- [19] M. M. Glazov, I. A. Yugova, S. Spatzek, A. Schwan, S. Varwig, D. R. Yakovlev, D. Reuter, A. D. Wieck, and M. Bayer, *Phys. Rev. B* **82**, 155325 (2010)
- [20] D. M. Gelmont B.L., *Fiz. Tekhn. Poluprov.* **5**, 2191 (1971) [Engl. transl: *Sov. Phys. Semicond.* **5**, 1905 (1972)]
- [21] A. Baldereschi and N. Lipari, *Phys. Rev. B* **8**, 2697 (1973)
- [22] A. L. Efros and A. Rodina, *Solid State Commun.* **72**, 645 (1989)
- [23] S. V. Goupalov, E. L. Ivchenko, and A. V. Kavokin, *JETP* **86**, 388 (1998)
- [24] *Optical Orientation*, edited by F. Meier and B. P. Zakharchenya (North Holland, Amsterdam, 1984)
- [25] A. L. Efros, *Phys. Rev. B* **46**, 7448 (1992)
- [26] E. A. Zhukov, D. R. Yakovlev, M. Bayer, M. M. Glazov, E. L. Ivchenko, G. Karczewski, T. Wojtowicz, and J. Kosut, *Phys. Rev. B* **76**, 205310 (2007)
- [27] I. A. Yugova, A. A. Sokolova, D. R. Yakovlev, A. Greilich, D. Reuter, A. D. Wieck, and M. Bayer, *Phys. Rev. Lett.* **102**, 167402 (2009)
- [28] I. A. Yugova, M. M. Glazov, D. R. Yakovlev, A. A. Sokolova, and M. Bayer, *Phys. Rev. B* **85**, 125304 (2012)
- [29] R. Binder and M. Lindberg, *Phys. Rev. B* **61**, 2830 (2000)
- [30] N. Janssen, K. M. Whitaker, D. R. Gamelin, and R. Bratschitsch, *Nano Letters* **8**, 1991 (2008)
- [31] M. Syperek, D. R. Yakovlev, I. A. Yugova, J. Misiewicz, I. V. Sedova, S. V. Sorokin, A. A. Toropov, S. V. Ivanov, and M. Bayer, *Phys. Rev. B* **84**, 085304 (2011)
- [32] J. M. Kikkawa and D. D. Awschalom, *Phys. Rev. Lett.* **80**, 4313 (1998)
- [33] A. Greilich, R. Oulton, E. A. Zhukov, I. A. Yugova, D. R. Yakovlev, M. Bayer, A. Shabaev, A. L. Efros, I. A. Merkulov, V. Stavarache, D. Reuter, and A. Wieck, *Phys. Rev. Lett.* **96**, 227401 (2006)
- [34] S. G. Carter, A. Shabaev, S. E. Economou, T. A. Kennedy, A. S. Bracker, and T. L. Reinecke, *Phys. Rev. Lett.* **102**, 167403 (2009)
- [35] M. M. Glazov, I. A. Yugova, and A. L. Efros, *Phys. Rev. B* **85**, 041303(R) (2012)
- [36] M. M. Glazov and E. L. Ivchenko, *Fiz. Tekhn. Poluprov.* **42**, 966 (2008) [Engl. transl.: *Semiconductors* **42**, 951 (2008)]
- [37] Linearly polarized pulse affects the electron spin polarization in the nanocrystal [8]. One can show that electron spin components before (\mathbf{S}^-) and after (\mathbf{S}^+) the linearly polarized pulse are related as $\mathbf{S}^+ = Q_l \mathbf{S}^-$, where, e.g. for resonant pulse, $Q_l = \cos^2(\Theta_l/\sqrt{2})$, there Θ_l is the linearly polarized pulse area.
- [38] In the linear in the \mathbf{E}^{pr} regime the probe-induced dielectric polarization does not contain contributions like $\{J_x \sigma_y\}_s$ as well.
- [39] H. Kosaka, T. Inagaki, Y. Rikitake, H. Imamura, Y. Mitsumori, and K. Edamatsu, *Nature* **457**, 702 (2009)
- [40] E. L. Ivchenko, *Optical Spectroscopy of Semiconductor Nanostructures* (Alpha Science, Harrow UK, 2005)
- [41] I. A. Yugova, A. Greilich, D. R. Yakovlev, A. A. Kiselev, M. Bayer, V. V. Petrov, Y. K. Dolgikh, D. Reuter, and A. D. Wieck, *Phys. Rev. B* **75**, 245302 (2007)